

## Chapter 2

### Imaging both sides of steeply dipping reflectors

Migration of both normal reflections (reflected from the topsides of steeply dipping reflectors) and overturned reflections (reflected from the undersides of steeply dipping reflectors) will improve resolution of these reflectors. Conventional migration usually treats overturned reflections as evanescent energy and ignores them when downward continuing the wavefield. To image both sides of steeply-dipping reflectors, a two-pass phase-shift extrapolation method, proposed by Claerbout, is used to migrate the normal and the overturned reflections separately (Li, Claerbout, and Ottolini, 1984). When velocity varies laterally, however, the phase-shift method is not appropriate. The problem of migrating steep-dip and overturned reflections in laterally inhomogeneous media has led to the formulation of a new wavefield extrapolation method, which will be derived in chapter 3.

#### § 2.1 OVERTURNED REFLECTIONS

Because the processing of overturned reflection data offers an image of the undersides of reflectors, this processing becomes important when we want to accurately determine the positions of steeply dipping reflectors. It is particularly important in determining salt-dome boundaries. When a seismic survey is conducted over a mushroom-shaped salt dome, as shown in Figure 2.1, it is observed that reflections from the topsides of steeply dipping flanks of the salt-dome are usually too weak, or too incoherent, to be recorded. The reasons for this weakness might be that the incident energy is trapped inside the salt dome because of the high reflectivity on the salt dome boundary, and that the normal reflections are highly attenuated and diffracted by the normal fault systems usually developed over the top of the salt dome. Therefore, the flanks of the mushroom-shaped salt domes are usually missing from the conventional migrated section. On the other hand, overturned reflections might be recorded because their ray paths are completely outside the salt dome. Thus, processing the overturned reflections may help us locate the flanks of the salt dome.

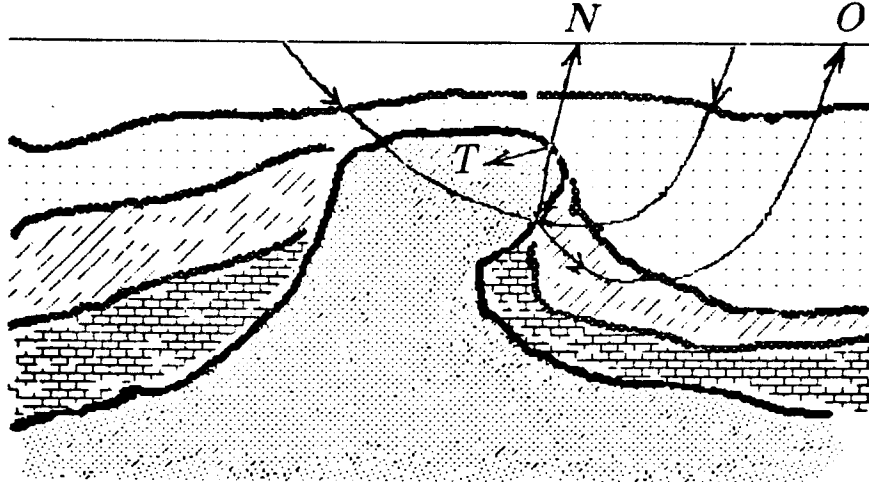


FIG. 2.1. Normal and overturned reflections over a salt dome. The normal reflection, N, is too weak to be recorded, because part of the energy, T, is trapped inside the salt dome. The overturned reflection, O, is recorded.

Processing the overturned reflections has other purposes: first, a comparison of the normal reflection image and the overturned reflection image may more accurately determine the locations of the dipping reflectors and the velocity distributions; second, combining these two images will better resolve the dipping reflectors.

## § 2.2 TWO-PASS PHASE-SHIFT MIGRATION

Migration by depth extrapolation is usually done by downward continuing the wavefield observed on the surface to various depths of exploration interest. Using the exploding reflector concept (Loewenthal et al., 1976), a zero-offset time section can be regarded as a seismogram which records waves that are generated from reflectors at time  $t = 0$  and propagated upwards with half of the medium velocity.

The downward depth extrapolation of the wavefield  $P(\omega, k_x, z)$  from depth  $z$  to depth  $z + \Delta z$  is based on the following equation:

$$P(\omega, k_x, z + \Delta z) = P(\omega, k_x, z) e^{ik_z \Delta z}, \quad (2.1)$$

where  $P(\omega, k_x, z)$  denotes the 2-D Fourier transform of the data  $P(t, x, z)$ ,  $v(z)$  is one-half of the medium velocity, and  $k_z$  is defined by

$$k_z = -\frac{\omega}{v(z)} \left( 1 - \frac{v^2(z)k_x^2}{\omega^2} \right)^{1/2}. \quad (2.2)$$

The square root in equation (2.2) must be real to extrapolate the propagating waves, because the extrapolated energy will decay or grow exponentially when the square root is imaginary. The extrapolation operator thus applies only to the region  $|vk_x/\omega| < 1$ , as depicted in Figure 2.2.

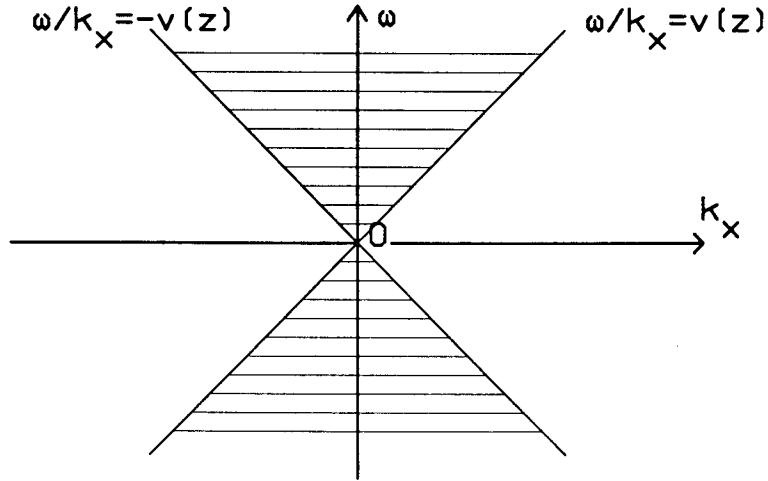


FIG. 2.2. Pie-slice diagram in the Fourier domain showing the region of wave propagation. The extrapolation operator  $\exp[-i\omega\Delta z \sqrt{1-v^2(z)k_x^2/\omega^2} / v(z)]$  applies only to the shaded region  $|vk_x/\omega| < 1$ .

The vertical component of the wavenumber  $k_z$  can be related to the frequency  $\omega$  and the angle of wave propagation  $\theta$  (between the direction of propagation and the vertical axis) by

$$k_z = \frac{\omega}{v(z)} \cos \theta. \quad (2.3)$$

Therefore, during the downward depth extrapolation, the angle of wave propagation is restricted to

$$\frac{\pi}{2} < |\theta| < \pi, \quad (2.4)$$

because, according to equation (2.2),  $\cos \theta$  must always be negative if the square root does not become imaginary. In other words, equations (2.1) and (2.2) will only extrapolate upcoming ( $\pi/2 < |\theta| < \pi$ ) wavefields specified in the region  $|vk_x/\omega| < 1$ , while the remaining energy, namely horizontally propagating waves and some surface

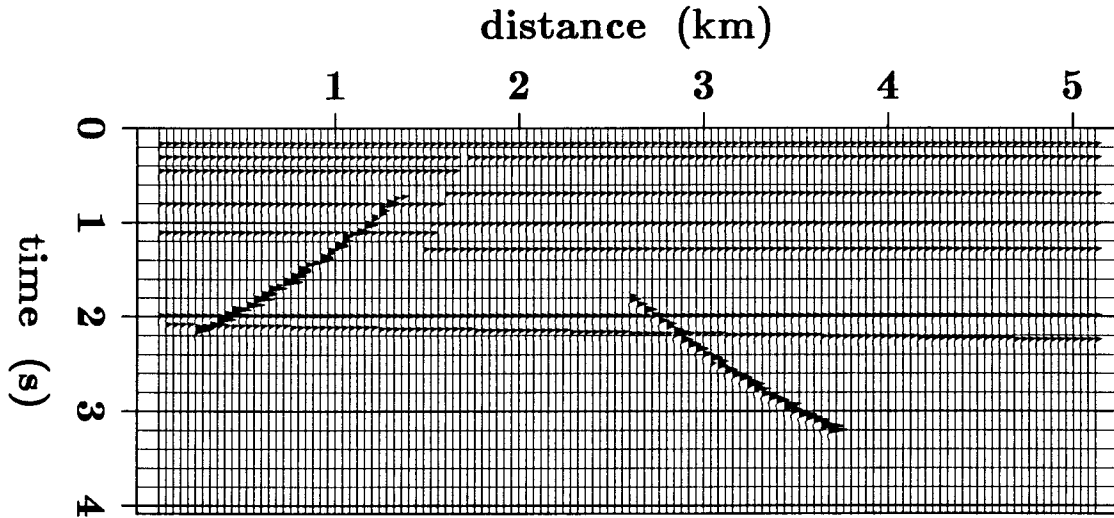
waves, stays in the region  $|vk_x/\omega| \geq 1$ , where the operator does not apply. The energy in the region  $|vk_x/\omega| \geq 1$  is usually called evanescent energy, because it decays exponentially with depth.

In zero-offset sections, the wavefield recorded at the earth's surface can contain both normal reflections, which have only upcoming ray paths, and overturned reflections, which contain both downgoing and upcoming ray paths (here the exploding reflector model is used again). The path of an overturned reflection can be divided into two subpaths: one going downward until it hits a turning point, where  $\theta = \pi/2$  or  $\theta = -\pi/2$ ; the other coming upward after the turning point. After applying downward extrapolation using equations (2.1) and (2.2), the normal reflections will be fully imaged at the corresponding reflector positions, while the overturned reflections are migrated only to the corresponding turning points, because the operator is not applied to the region where  $|\theta| \leq \pi/2$ . Conventional phase-shift migration stops at this stage, producing the images of normal reflections.

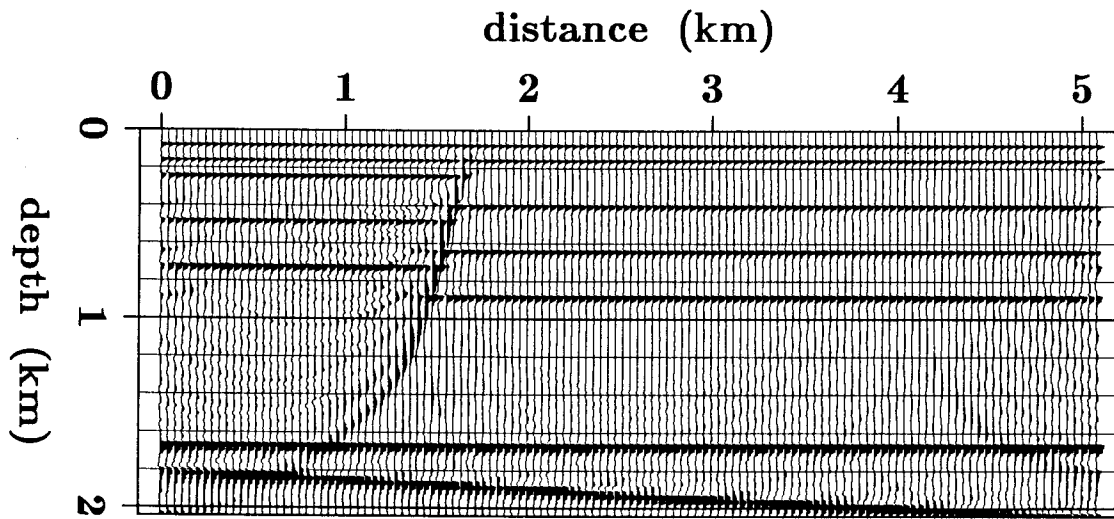
Can we make use of the overturned reflections that have already been migrated to the turning points? Yes, if we do a second pass extrapolation, i.e., upward extrapolation. With upward extrapolation we will be able to continue migrating the overturned reflections beyond the turning points and upward to the reflector positions. As a result of migrating overturned reflections, we obtain another image of the subsurface structure.

Two-pass phase-shift migration can thus be summarized in two steps: (1) apply conventional downward extrapolation and save the overturned energy at the turning points; (2) apply upward extrapolation to the energy saved in the first pass of continuation. Thus, two-pass migration yields one image of the normal reflection and another of the overturned reflection. A modified version of Claerbout's two-pass phase-shift algorithm (Claerbout, 1985) is given in Appendix 1.

Figure 2.3 shows the result of applying two-pass phase-shift migration to a synthetic zero-offset section. The two different images of the overthrust fault plane are positioned exactly at the same proper place. Combining these two results together gives a stronger indication of the fault plane in Figure 2.3d than the conventional downward extrapolation result shown in Figure 2.3b.

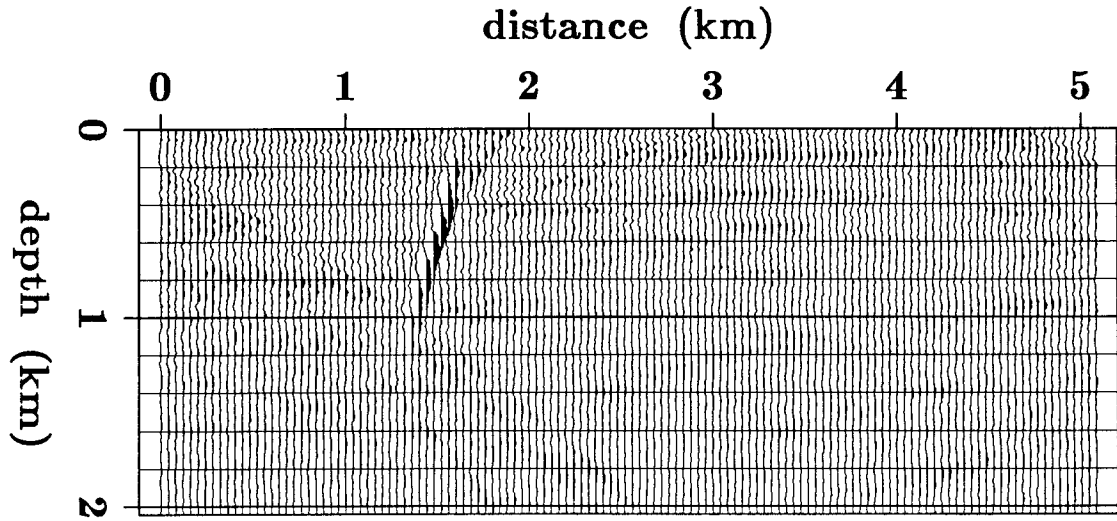


**a**

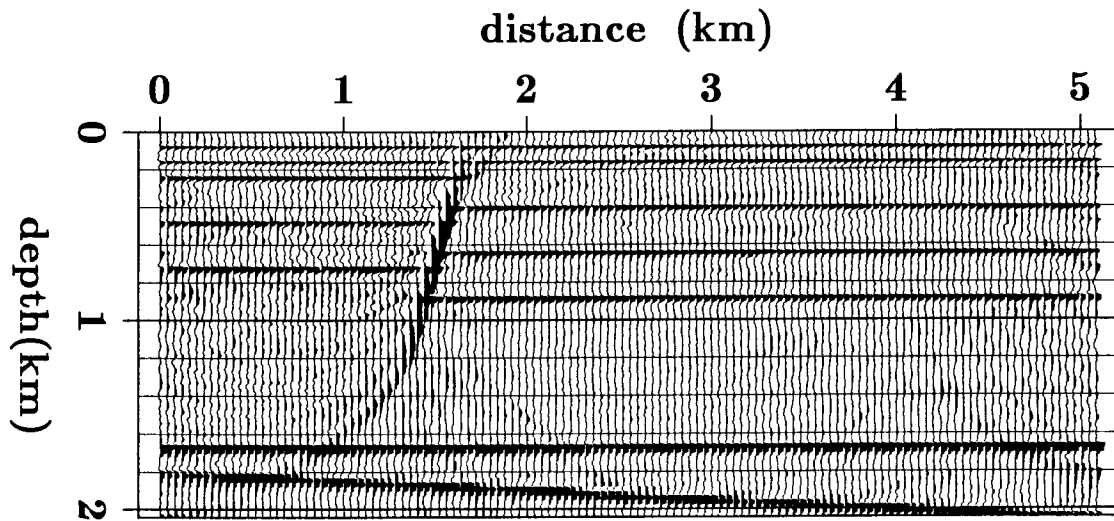


**b**

FIG. 2.3. **a.** Synthetic zero-offset seismogram of a model of a thrust fault system with a 75-degree dipping fault plane. The velocity of the model is given by  $v(z)=1+z$  (km/s). The normal reflection of the fault plane is shown on the upper left. The overturned reflection of the fault plane is on the lower right. A ray tracing method is used to compute the seismogram, which is only kinematically correct. **b.** Migrated depth section after first pass of downward extrapolation.



**c**



**d**

FIG. 2.3. **c.** Migrated depth section after two-pass extrapolation. **d.** Final migrated depth section produced by combining the two images in Figures 2.3b and 2.3c. The fault-plane image has been significantly enhanced.

### § 2.3 RECORDING AND STACKING OVERTURNED REFLECTIONS

It has been shown that two-pass phase-shift migration can be used to image both normal and overturned reflections. However, overturned reflections are rarely identified and interpreted in the seismic exploration industry, because several difficulties exist relating to both acquisition and processing of overturned reflection data.

Overturned reflections usually travel longer distances and arrive later than normal reflections. Therefore, conventional data-acquisition techniques, typically with receiver cables of a few kilometers and recording times of six seconds, may not be able to record them. The larger the angle of a reflector is, the shorter the cable length and recording time that are needed to record overturned reflections from the reflector. Large velocity gradients also reduce their traveling distances and arrival times. Positions of sources and receivers with respect to dipping reflectors are other important factors in recording these reflections. Synthetic ray tracing of reflections (see Appendix 2) will be helpful in designing field data-acquisition techniques to record overturned reflections.

Ray-tracing results in constant-velocity-gradient media (see Appendix 2) show that the travel-time curves of overturned and normal reflections have opposite curvatures in common-shot gathers. Therefore, overturned and normal reflections can be separated and stacked (by slant stack) into two different sections by using their slope (or curvature) differences in the common-shot gathers.

It is well known that the travel-time curves of normal reflections have positive moveout corrections in common-midpoint gathers; i.e., travel time increases as offsets between source and receiver increase. However, synthetic ray-tracing results show that the travel-time curves of overturned reflections have negative moveout corrections in common-midpoint gathers. Therefore, we can apply negative moveout correction to common-midpoint gathers to stack overturned reflections into one section, while stacking normal reflections into another section by applying normal (positive) moveout corrections to the gathers.

Data aliasing caused by insufficient sampling in CMP gathers can make stacking over CMP gathers difficult. The aliasing effect can be avoided or reduced if we do slant stacking in common shot gathers (CSG), in case where the trace interval is smaller in the common-shot gather than in the CMP gather. Since overturned reflections and normal reflections have opposite curvatures in shot gathers, over a certain range of the offsets the two reflections can be stacked into different sections according to their slopes.

Stacking common-midpoint gathers or shot profiles has the effect of averaging reflectivities over certain segments of reflectors, because coherent overturned reflections in CMP or CSG gathers do not originate from a single reflection point. To overcome this problem, two-way prestack migration should be used. Prestack migration using a two-way wave equation will be discussed in chapter 5.

#### § 2.4 MIGRATION OF OVERTURNED REFLECTIONS IN LATERALLY INHOMOGENEOUS MEDIA

Two-pass Fourier-domain phase-shift migration is not valid when the velocity of the medium is laterally varying. Migration, then, has to be carried out in the physical domain  $(t, x, z)$  or  $(\omega, x, z)$ . To preserve the accuracy of migration, the LITWEQ method was developed. This new migration method has the economy of the conventional finite-difference migration methods, yet is accurate for reflections of any propagating angle. One application of the LITWEQ method is the migration of overturned reflections. The two-way property and the high accuracy of LITWEQ make LITWEQ migration of overturned waves possible.

Figure 2.4 shows two images of a fault plane after applying LITWEQ migration to a zero-offset section of a normal reflection and a zero-offset section of an overturned reflection. However, like reverse time migration (Baysal et al., 1984), LITWEQ can only offer one image if both normal and overturned reflections are stacked into a single section, because both reflections are migrated simultaneously and merged at the reflector positions.

Figure 1.2 showed a result of applying LITWEQ migration to a field dataset that contained reflections from flanks of a mushroom-shaped salt dome. The reflections from the overhanging side of the dome were overturned. The LITWEQ method images these reflections, as shown in Figure 1.2.

The principles and applications of the LITWEQ method will be discussed in detail in the coming chapters.



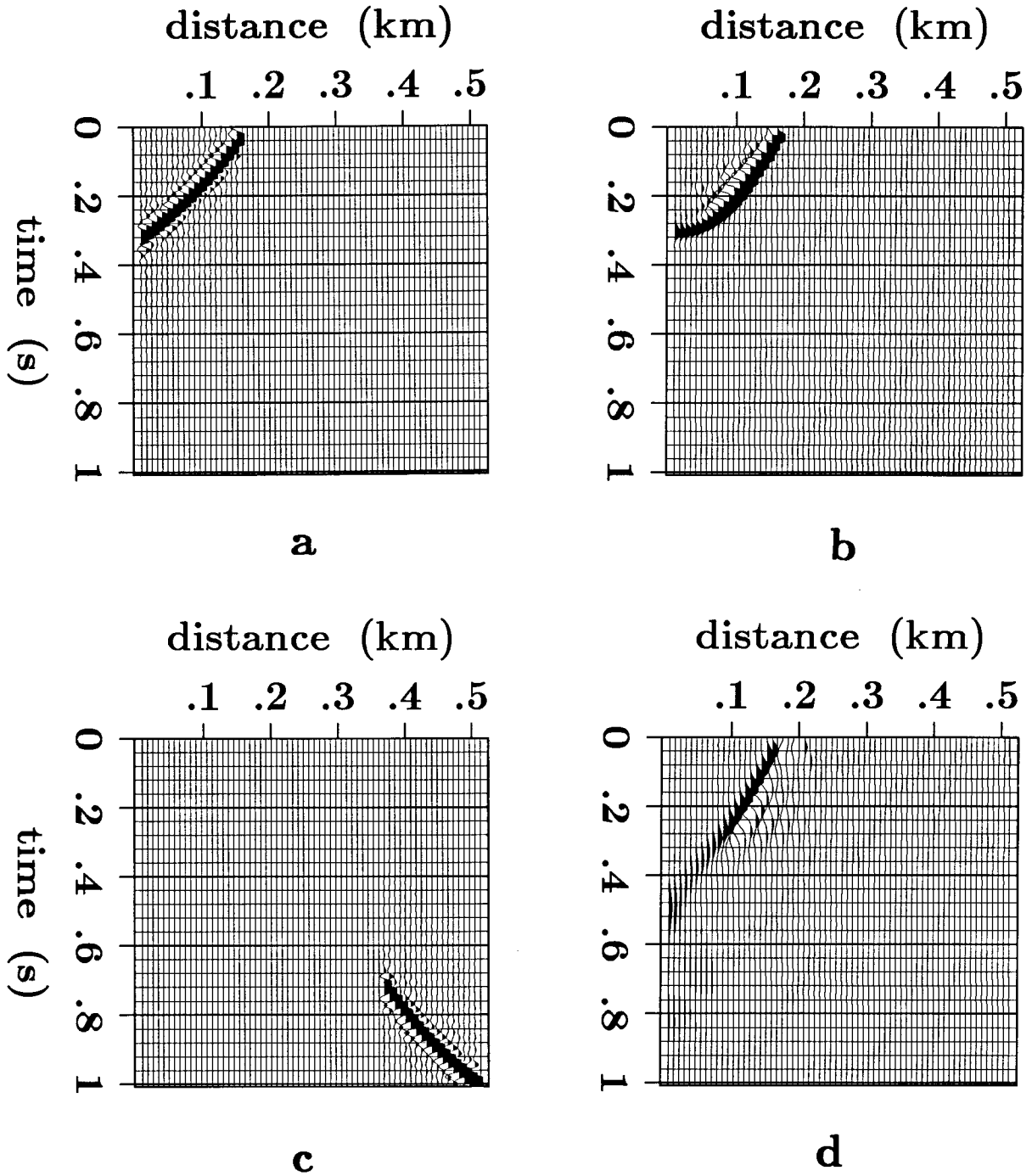


FIG. 2.4. **a.** Zero-offset section for a normal reflection generated from the topside of a 45-degree dipping fault plane. **b.** Result of applying LITWEQ migration to Figure 2.4a. The image of the topside of the fault plane is obtained by migrating the normal reflection. **c.** Zero-offset section for an overturned reflection generated from the underside of the same fault plane as in Figure 2.4a. **d.** Result of applying LITWEQ migration to Figure 2.4c. The image of the underside of the fault plane is obtained by migrating the overturned reflection.

## § 2.5 SUMMARY

Large-angle and overturned reflections can be migrated by two-pass phase-shift migration, when the velocity of the medium is a function of depth only. Ray-tracing techniques can help in designing special field data-acquisition methods for recording overturned reflections. When the velocity gradient is constant, negative moveout correction in CMP gathers must be applied before overturned reflections can be stacked into zero-offset sections.

To solve the problem of imaging both sides of steeply dipping reflectors in laterally inhomogeneous media, the LITWEQ wavefield extrapolation method is proposed. The finite-difference LITWEQ migration method can image both normal and overturned reflections in laterally inhomogeneous media.

Because the Stanford Research Project has limited access to field data and is not able to conduct a field survey using specially designed data-acquisition techniques, solutions to the problem of imaging both the topsides and undersides of steeply dipping reflectors are still theoretical. Industry people should be able to continue this work and apply theoretical solutions to field data processing of overturned reflections.